Bioinformatics sequence analysis

Multiple sequence alignments of kinase domains in the human kinome were performed for 321 human kinase domains. The positions of the conserved glutamate (E) and arginine (R) residues are colored purple and those of EGFR are indicated in red. FASTA files for human kinase domains were obtained from the kinase database at Sugen/Salk (Kinbase, La Jolla, CA, USA) and aligned with the AliBee multiple sequence alignment program (GeneBee) (Brodsky *et al.*, 1992) using Clustal format. Resulting alignments were colored using JalView 2.2 (Clamp *et al.*, 2004) according to sequence conservation (BLOSUM62). In addition, the amino-acid sequences from a selected list of 32 diverse human protein kinases were obtained from the ENSEMBL database (www.ensembl.org). The amino-acid sequences of these kinase domains were analysed and aligned using the EMBL-EBI online CLUSTALW software (www.ebi.ac.uk/clustalw).

Structural analysis

EGFR crystal structures (PDB accession codes 1M17, 1XKK and 2GS6) (Stamos *et al.*, 2002; Wood *et al.*, 2004; Zhang *et al.*, 2006) were analysed using the program O (Jones *et al.*, 1991). Superposition of the EGFR kinase domain with the catalytic domains of diverse kinases was performed to study the structural conservation of a buried Glu(E)–Arg(R) ion pair. The crystal structure of EGFR tyrosine kinase (PDB accession code: 1M17) (Stamos *et al.*, 2002) was superimposed with the catalytic kinase domains of human CDK2 (PDB accession code: 1VYW) (Pevarello *et al.*, 2004), human JNK3 (PDB accession code: 1PMQ) (Scapin *et al.*, 2003), human insulin receptor kinase (PDB accession code: 1IR3) (Hubbard, 1997), ZAP-70 tyrosine kinase (PDB accession code: 1U59) (Jin *et al.*, 2004), LCK kinase (PDB accession code: 1QPD) (Zhu *et al.*, 1999) and MET (PDB accession code: 2RFS) (Bellon *et al.*, 2008) using Cα atoms in the program DeepView/Swiss-PdbViewer v3.7. Figures were prepared using the program PYMOL (www.pymol.org).

Abbreviations

COSMIC, catalogue of somatic mutations in cancer; EGFR, epidermal growth factor receptor; MAPK (ERK1/2), mitogen-activated protein kinase (extracellular signaling-regulated kinase 1/2); STAT3, signal transducer and activator of transcription 3; TKI, tyrosine kinase inhibitor.

Acknowledgements

Patrick C Ma is supported by NIH/National Cancer Institute-K08 Career Development Award (5K08CA102545-04), American Cancer Society (Ohio)-Institutional Research Grant (IRG-91-022, Case Comprehensive Cancer Center) and Ohio Cancer Research Associates (Give New Ideas A Chance) Grant Award. Titus J Boggon is an American Society of Hematology Junior Faculty Scholar. Edward T Petri is supported by an NIH/National Cancer Institute T32 training Grant (5T32CA009085-32). We thank Dr Zhenghe J Wang (Department of Genetics, Case Western Reserve University) for critically reading the manuscript and for helpful suggestions.

References

Bean J, Brennan C, Shih JY, Riely G, Viale A, Wang L *et al.* (2007). MET amplification occurs with or without T790M mutations in EGFR mutant lung tumors with acquired resistance to gefitinib or erlotinib. *Proc Natl Acad Sci USA* **104**: 20932 20937.

Bellon SF, Kaplan-Lefko P, Yang Y, Zhang Y, Moriguchi J, Rex K *et al.* (2008). c-Met inhibitors with novel binding mode show activity against several hereditary papillary renal cell carcinoma related mutations. *J Biol Chem* **283**: 2675 2683.

Brodsky LI, Vasiliev AV, Kalaidzidis YL, Osipov YS, Tatuzov RL, Feranchuk SI. (1992). GeneBee: the program package for biopolymer structure analysis. *Dimacs* **8**: 127 139.

Chen Z, Feng J, Saldivar JS, Gu D, Bockholt A, Sommer SS (2008). EGFR somatic doublets in lung cancer are frequent and generally arise from a pair of driver mutations uncommonly seen as singlet mutations: one-third of doublets occur at five pairs of amino acids. *Oncogene* **27**: 4336 4343.

Choong NW, Dietrich S, Seiwert TY, Tretiakova MS, Nallasura V, Davies GC *et al.* (2006). Gefitinib response of erlotinib-refractory lung cancer involving meninges—role of EGFR mutation. *Nat Clin Pract Oncol* **3**: 50 57; quiz 51 p following 57.

Clamp M, Cuff J, Searle SM, Barton GJ. (2004). The Jalview Java alignment editor. *Bioinformatics* **20**: 426 427.

Di Renzo MF, Olivero M, Martone T, Maffe A, Maggiora P, Stefani AD *et al.* (2000). Somatic mutations of the MET oncogene are selected during metastatic spread of human HNSC carcinomas. *Oncogene* **19**: 1547 1555.

Engelman JA, Zejnullahu K, Mitsudomi T, Song Y, Hyland C, Park JO *et al.* (2007). MET amplification leads to gefitinib resistance in lung cancer by activating ERBB3 signaling. *Science* **316**: 1039 1043.

Frohling S, Scholl C, Levine RL, Loriaux M, Boggon TJ, Bernard OA *et al.* (2007). Identification of driver and passenger mutations of FLT3 by high-throughput DNA sequence analysis and functional assessment of candidate alleles. *Cancer Cell* **12**: 501 513.

Guo A, Villen J, Kornhauser J, Lee KA, Stokes MP, Rikova K *et al.* (2008). Signaling networks assembled by oncogenic EGFR and c-Met. *Proc Natl Acad Sci USA* **105**: 692 697.

Hubbard SR. (1997). Crystal structure of the activated insulin receptor tyrosine kinase in complex with peptide substrate and ATP analog. *Embo J* **16**: 5572 5581.

Jackman DM, Holmes AJ, Lindeman N, Wen PY, Kesari S, Borras AM *et al.* (2006). Response and resistance in a non-small-cell lung cancer patient with an epidermal growth factor receptor mutation and leptomeningeal metastases treated with high-dose gefitinib. *J Clin Oncol* **24**: 4517 4520.

Jagadeeswaran R, Ma PC, Seiwert TY, Jagadeeswaran S, Zumba O, Nallasura V *et al.* (2006). Functional analysis of c-Met/hepatocyte growth factor pathway in malignant pleural mesothelioma. *Cancer Res* **66**: 352 361.

Ji H, Ramsey MR, Hayes DN, Fan C, McNamara K, Kozlowski P *et al.* (2007). LKB1 modulates lung cancer differentiation and metastasis. *Nature* **448**: 807 810.

Jin L, Pluskey S, Petrella EC, Cantin SM, Gorga JC, Rynkiewicz MJ *et al.* (2004). The three-dimensional structure of the ZAP-70 kinase domain in complex with staurosporine: implications for the design of selective inhibitors. *J Biol Chem* **279**: 42818 42825.

Jones TA, Zou JY, Cowan SW, Kjeldgaard M. (1991). Improved methods for building protein models in electron density maps and the location of errors in these models. *Acta Crystallogr A* **47**(Part 2): 110 119.

Kobayashi S, Boggon TJ, Dayaram T, Janne PA, Kocher O, Meyerson M *et al.* (2005). EGFR mutation and resistance of non-small-cell lung cancer to gefitinib. *N Engl J Med* **352**: 786 792.

Krause DS, Van Etten RA. (2005). Tyrosine kinases as targets for cancer therapy. *N Engl J Med* **353**: 172 187.

Lo HW, Hsu SC, Ali-Seyed M, Gunduz M, Xia W, Wei Y *et al.* (2005). Nuclear interaction of EGFR and STAT3 in the activation of the iNOS/NO pathway. *Cancer Cell* **7**: 575 589.

Lynch TJ, Bell DW, Sordella R, Gurubhagavatula S, Okimoto RA, Brannigan BW *et al.* (2004). Activating mutations in the epidermal growth factor receptor underlying responsiveness of non-small-cell lung cancer to gefitinib. *N Engl J Med* **350**: 2129 2139.

Ma PC, Jagadeeswaran R, Jagadeesh S, Tretiakova MS, Nallasura V, Fox EA *et al.* (2005a). Functional expression and mutations of c-Met and its therapeutic inhibition with SU11274 and small interfering RNA in non-small cell lung cancer. *Cancer Res* **65**: 1479 1488.

Ma PC, Kijima T, Maulik G, Fox EA, Sattler M, Griffin JD *et al.* (2003a). c-MET mutational analysis in small cell lung cancer: novel juxtamembrane domain mutations regulating cytoskeletal functions. *Cancer Res* **63**: 6272 6281.

Ma PC, Maulik G, Christensen J, Salgia R. (2003b). c-Met: structure, functions and potential for therapeutic inhibition. *Cancer Metastasis Rev* **22**: 309 325.

Ma PC, Schaefer E, Christensen JG, Salgia R. (2005b). A selective small molecule c-MET Inhibitor, PHA665752, cooperates with rapamycin. *Clin Cancer Res* **11**: 2312 2319.

Ma PC, Tretiakova MS, Nallasura V, Jagadeeswaran R, Husain AN, Salgia R. (2007). Downstream signalling and specific inhibition of c-MET/HGF pathway in small cell lung cancer: implications for tumour invasion. *Br J Cancer* **97**: 368 377.

Mazzone M, Comoglio PM. (2006). The Met pathway: master switch and drug target in cancer progression. *FASEB J* **20**: 1611 1621.

Paez JG, Janne PA, Lee JC, Tracy S, Greulich H, Gabriel S *et al.* (2004). EGFR mutations in lung cancer: correlation with clinical response to gefitinib therapy. *Science* **304**: 1497 1500.

Peruzzi B, Bottaro DP. (2006). Targeting the c-Met signaling pathway in cancer. *Clin Cancer Res* **12**: 3657 3660.

Pevarello P, Brasca MG, Amici R, Orsini P, Traquandi G, Corti L *et al.* (2004). 3-Aminopyrazole inhibitors of CDK2/cyclin A as antitumor agents. 1. Lead finding. *J Med Chem* **47**: 3367 3380.

Rikova K, Guo A, Zeng Q, Possemato A, Yu J, Haack H *et al.* (2007). Global survey of phosphotyrosine signaling identifies oncogenic kinases in lung cancer. *Cell* **131**: 1190 1203.

Scapin G, Patel SB, Lisnock J, Becker JW, LoGrasso PV. (2003). The structure of JNK3 in complex with small molecule inhibitors: structural basis for potency and selectivity. *Chem Biol* **10**: 705 712.

Shigematsu H, Gazdar AF. (2006). Somatic mutations of epidermal growth factor receptor signaling pathway in lung cancers. *Int J Cancer* **118**: 257 262.

Shinomiya N, Gao CF, Xie Q, Gustafson M, Waters DJ, Zhang YW *et al.* (2004). RNA interference reveals that ligand-independent met activity is required for tumor cell signaling and survival. *Cancer Res* **64**: 7962 7970.

Smolen GA, Sordella R, Muir B, Mohapatra G, Barmettler A, Archibald H *et al.* (2006). Amplification of MET may identify a subset of cancers with extreme sensitivity to the selective tyrosine kinase inhibitor PHA-665752. *Proc Natl Acad Sci USA* **103**: 2316 2321.

Stamos J, Sliwkowski MX, Eigenbrot C. (2002). Structure of the epidermal growth factor receptor kinase domain alone and in complex with a 4-anilinoquinazoline inhibitor. *J Biol Chem* **277**: 46265 46272.

Tam IY, Chung LP, Suen WS, Wang E, Wong MC, Ho KK *et al.* (2006). Distinct epidermal growth factor receptor and KRAS mutation patterns in non-small cell lung cancer patients with different tobacco exposure and clinicopathologic features. *Clin Cancer Res* **12**: 1647 1653.

Tang Z, Du R, Jiang S, Wu C, Barkauskas DS, Richey J *et al.* (2008). Dual MET-EGFR combinatorial inhibition against T790M-EGFR-mediated erlotinib-resistant lung cancer. *Br J Cancer* **99**: 911 922, 2008.

Thomas RK, Baker AC, Debiasi RM, Winckler W, Laframboise T, Lin WM *et al.* (2007). High-throughput oncogene mutation profiling in human cancer. *Nat Genet* **39**: 347 351.

Wood ER, Truesdale AT, McDonald OB, Yuan D, Hassell A, Dickerson SH *et al.* (2004). A unique structure for epidermal growth factor receptor bound to GW572016 (Lapatinib): relationships among protein conformation, inhibitor off-rate, and receptor activity in tumor cells. *Cancer Res* **64**: 6652 6659.

Zhang X, Gureasko J, Shen K, Cole PA, Kuriyan J. (2006). An allosteric mechanism for activation of the kinase domain of epidermal growth factor receptor. *Cell* **125**: 1137 1149.

Zhu X, Kim JL, Newcomb JR, Rose PE, Stover DR, Toledo LM *et al.* (1999). Structural analysis of the lymphocyte-specific kinase Lck in complex with non-selective and Src family selective kinase inhibitors. *Structure* **7**: 651 661.

Supplementary Information accompanies the paper on the Oncogene website (http://www.nature.com/onc)

Large Cell Neuroendocrine Carcinoma of the Mediastinum with α-Fetoprotein Production

Ken Takezawa, MD, Isamu Okamoto, MD, PhD,* Junya Fukuoka, MD, PhD,† Kaoru Tanaka, MD,* Hiroyasu Kaneda, MD,* Hisao Uejima, MD,‡ Hyung-Eun Yoon, MD, PhD,‡ Masami Imakita, MD, PhD,§ Masahiro Fukuoka, MD, PhD,* and Kazuhiko Nakagawa, MD, PhD**

Large cell neuroendocrine carcinoma (LCNEC) is a relatively new category of pulmonary neuroendocrine tumor. Although it was first detected in the lung, LCNEC has since been found in a variety of extrapulmonary sites. We now describe a patient who was diagnosed with LCNEC originating from the mediastinum, an extremely rare disorder. An increased serum concentration of α-fetoprotein (AFP) in the patient was reduced by chemotherapy in association with tumor shrinkage. Furthermore, the tumor was confirmed immunohistochemically to produce AFP. To our knowledge, this is the first report of a LCNEC that produces AFP.

Key Words: Large cell neuroendocrine carcinoma, α-Fetoprotein, Mediastinal tumor.

(*J Thorac Oncol.* 2008;3: 187–189)

Large cell neuroendocrine carcinoma (LCNEC) is a high-grade neuroendocrine tumor that was first detected in the lung by Travis et al.[1] The prognosis of individuals with LCNEC has been reported to be poor, with a 5-year survival rate similar to that for small cell carcinoma.[2–4] Although originally found in the lung, LCNEC has since been described in a variety of extrapulmonary locations.[5–7] Among these locations, mediastinal LCNEC is extremely rare, with only a few cases having been reported.[8,9] We now report the first case of mediastinal LCNEC with α-fetoprotein (AFP) production.

CASE REPORT

A previously healthy 35-year-old Japanese man was found to have an abnormal mass in his right mediastinum on a chest radiograph during a health checkup. The patient's general condition was fair, and symptoms such as chest pain, weight loss, or fever were not noted. He was a current smoker, having smoked 20 cigarettes a day for 15 years. Computed tomography imaging of the chest revealed a 65 × 50 mm mass in the middle mediastinum (Figure 1*A*). Serum laboratory data were within normal limits. A bronchoscopic examination revealed a compression against the outside of the trachea. No other organs appeared to be affected on extensive examination. Subsequent evaluation for serum tumor markers revealed an increased level of AFP. Other examined markers, including β-human chorionic gonadotropin, carcinoembryonic antigen, and CA19-9, were within normal limits. Thoracoscopic examination revealed that the tumor was not invading into the adjacent lung. On the basis of these findings, we considered the tumor to have originated from the middle mediastinum. A biopsy revealed poorly differentiated carcinoma with neuroendocrine features. Thymic neuroendocrine carcinoma is exclusively located in the anterior-superior mediastinum.[1] Given the tumor's location, the increase in the serum concentration of AFP, and the patient's young age, the diagnosis of embryonal carcinoma was initially favored over purely neuroendocrine neoplasm.[1] The patient received neoadjuvant chemotherapy with bleomycin (30 mg/body) on days 2, 9, and 16, etoposide (100 mg/m^2) on days 1 to 5, and cisplatin (20 mg/m^2) on days 1 to 5. Treatment cycles were repeated every 21 days for 4 cycles. The serum AFP level had decreased to within normal limits in association with shrinkage of the tumor by the end of the third cycle of chemotherapy (Figure 1*B*, *E*). However, the AFP concentration started to increase thereafter, and progression of the tumor was confirmed after the fourth cycle of chemotherapy (Figure 1*C*, *E*). The patient then received second-line chemotherapy with cisplatin (80 mg/m^2) on day 1 and paclitaxel (200 mg/m^2) on day 1 every 21 days for three cycles before surgery. The serum AFP level again decreased in association with tumor shrinkage (Figure 1*D*, *E*). Eight months after initial detection of the tumor, the patient underwent a tumorectomy combined with right upper lobectomy and tracheoplasty, given that the tumor was found to invade the adjacent right upper lobe and trachea at the time of surgery. Histopathologic examination of the surgical specimen revealed a solid tumor nest with massive necrosis. The tumor was relatively homogeneous throughout the resection, showing sheets of cells with a high nucleus-to-cytoplasm ratio. High-power magnification of the tumor revealed that the tumor cells manifested marked neu-

*Department of Medical Oncology, Kinki University School of Medicine, Osaka; †Laboratory of Pathology, Toyama University Hospital, Toyama; ‡Division of Respirology; and §Division of Pathology, Rinku General Medical Center, Osaka, Japan.

Disclosure: The authors declare no conflict of interest.

Address for correspondence: Isamu Okamoto, MD, PhD, Department of Medical Oncology, Kinki University School of Medicine, 377-2 Ohno-higashi, Osaka-Sayama, Osaka 589-8511. E-mail: chi-okamoto@dotd.med.kindai.ac.jp

ISSN: 1556-0864/08/0302-0187

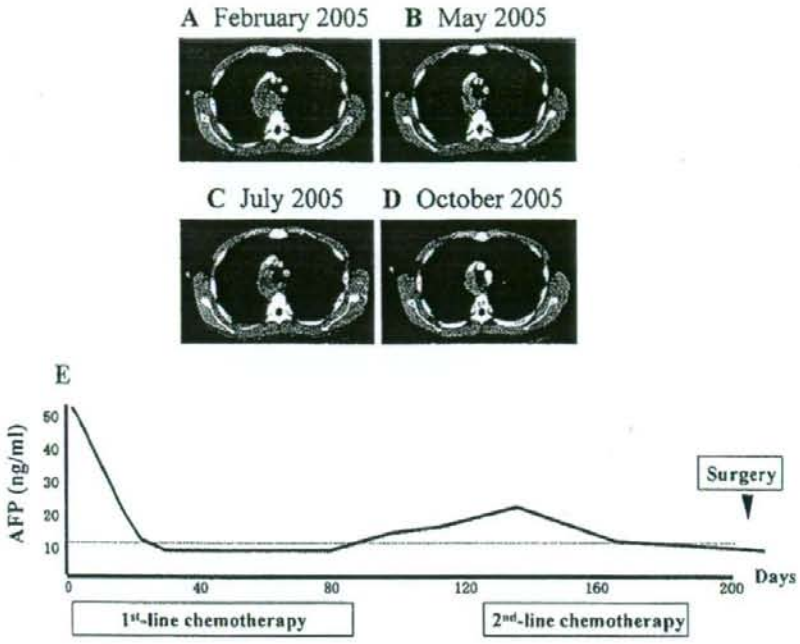

FIGURE 1. Chest computed tomography (CT) findings and serum AFP levels in the patient. *A–D*, Chest CT findings. A mass in the middle mediastinum was initially detected (*A*). The tumor had shrunk after three cycles of neoadjuvant chemotherapy (*B*), but its progression had resumed after the fourth cycle (*C*). The tumor shrank again in response to second-line chemotherapy (*D*). *E*, Time course of the serum concentration of AFP. The AFP level was initially increased, it decreased to within normal limits (dotted line) in association with tumor shrinkage during first-line chemotherapy, but it started to increase again after the third cycle. The serum AFP level again decreased in association with tumor shrinkage during second-line chemotherapy.

roendocrine features, such as frequent rosette structures and trabecular arrangements, nuclear moldings, and prominent mitoses (Figure 2*A*, *B*). The tumor cells also had abundant nucleoli. Immunohistochemical analysis showed the tumor cells to be diffusely positive for CK7 and neuroendocrine markers including CD56, chromogranin A (Figure 2*C*), and synaptophysin as well as negative for CD5, CD30, human chorionic gonadotropin, placental alkaline phosphatase, hepatocyte antigen, and thyroid transcription factor-1. No regions of the specimen showed features of a germ cell tumor or hepatoid carcinoma. On the basis of the morphology and staining characteristics of the tumor, a pathologic diagnosis of LCNEC was made. A small number of tumor cells showed subtle but unequivocal positive staining for AFP (Figure 2*D*). Thoracic radiotherapy was not able to be given because the patient suffered from thoracic empyema after surgery. Despite intensive chemotherapy, he died of extensive recurrence of carcinoma 4 months after the surgery.

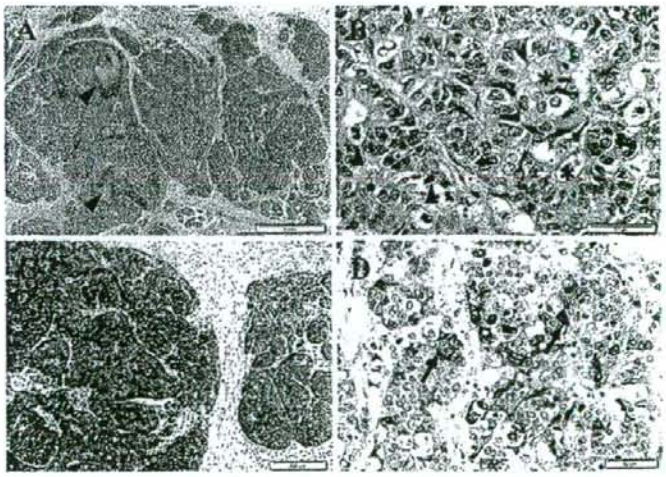

FIGURE 2. Histology and immunohistochemical analysis of the tumor specimen obtained at surgery. *A*, Hematoxylin-eosin staining revealed solid tumor nests with areas of necrosis (arrow heads). Note the homogeneous appearance of the tumor. *B*, High-power magnification of the tumor stained as in (*A*), showing numerous rosettes (asterisk), abundant cytoplasm, chromatin clearing with occasionally prominent nucleoli, nuclear molding (arrows), and frequent mitosis (arrow heads). *C*, Immunohistochemical staining for chromogranin A revealed diffuse and intense cytoplasmic staining. *D*, Immunohistochemical staining for AFP, showing a focus of tumor cells positive for AFP (arrows). Scale bars: 1 mm, 50 μ.

DISCUSSION

LCNEC is a relatively new category of pulmonary neuroendocrine tumor, with affected individuals reported to have a prognosis intermediate between those with atypical carcinoid lung cancer and those with small cell lung cancer.[10] Recent clinical studies indicate a 5-year survival rate of 27 to 67% even if patients are at pathologic stage I.[2–4] Since its original detection in the lung, LCNEC has been found in a variety of extrapulmonary locations including gastrointestinal sites and the uterine cervix.[5–7] The present case was identified as LCNEC originating in the mediastinum. Given the age of the patient and the tumor location, a diagnosis of embryonal carcinoma was initially considered, but no morphologic or immunohistochemical features indicative of embryonal carcinoma were found on extensive pathologic analysis of the surgical specimen. Primary mediastinal LCNEC is an extremely rare disorder and has been described in only a few case reports to date.[8–9]

In the present case, the increased serum AFP level decreased in association with tumor shrinkage in response to chemotherapy, and the tumor was confirmed immunohistochemically to produce AFP. AFP is the main component of fetal serum in mammals. It is synthesized by visceral endoderm of the yolk sac and fetal liver, but expression of the *AFP* gene is greatly reduced at the time of birth. AFP-producing carcinoma has been recognized for decades and reported in various locations including the lung and mediastinum.[11] In contrast to the present case, however, most cancers that produce AFP show morphologic features similar to hepatocellular carcinoma. With regard to neuroendocrine tumors, some case reports indicate that small cell carcinoma can also produce AFP.[12,13] As far as we are aware, however, the present case is the first reported example of LCNEC producing AFP. Given that the concept of LCNEC is relatively new, this may not be that surprising, and previous reports of small cell carcinoma may actually have been diagnosed as LCNEC today. Our case raises the possibility that the origin of mediastinal neuroendocrine tumors including LCNEC may be mediastinal primordial germ cells. Examination of germ cell tumor markers in neuroendocrine tumors may shed light on this matter.

REFERENCES

1. Travis WD, Linnoila RI, Tsokos MG, et al. Neuroendocrine tumors of the lung with proposed criteria for large-cell neuroendocrine carcinoma. An ultrastructural, immunohistochemical, and flow cytometric study of 35 cases. *Am J Surg Pathol* 1991;15:529–553.
2. Iyoda A, Hiroshima K, Toyozaki T, et al. Clinical characterization of pulmonary large cell neuroendocrine carcinoma and large cell carcinoma with neuroendocrine morphology. *Cancer* 2001;91:1992–2000.
3. Takei H, Asamura H, Maeshima A, et al. Large cell neuroendocrine carcinoma of the lung: a clinicopathologic study of eighty-seven cases. *J Thorac Cardiovasc Surg* 2002;124:285–292.
4. Travis WD, Rush W, Flieder DB, et al. Survival analysis of 200 pulmonary neuroendocrine tumors with clarification of criteria for atypical carcinoid and its separation from typical carcinoid. *Am J Surg Pathol* 1998;22:934–944.
5. Jiang SX, Mikami T, Umezawa A, et al. Gastric large cell neuroendocrine carcinomas: a distinct clinicopathologic entity. *Am J Surg Pathol* 2006;30:945–953.
6. Selvakumar E, Vimalraj V, Rajendran S, et al. Large cell neuroendocrine carcinoma of the ampulla of Vater. *Hepatobiliary Pancreat Dis Int* 2006;5:465–467.
7. Tangjitgamol S, Manusirivithaya S, Choomchuay N, et al. Paclitaxel and carboplatin for large cell neuroendocrine carcinoma of the uterine cervix. *J Obstet Gynaecol Res* 2007;33:218–224.
8. Chetty R, Batitang S, Govender D. Large cell neuroendocrine carcinoma of the thymus. *Histopathology* 1997;31:274–276.
9. Nagata Y, Ohno K, Utsumi T, et al. Large cell neuroendocrine thymic carcinoma coexisting within large WHO type AB thymoma. *Jpn J Thorac Cardiovasc Surg* 2006;54:256–259.
10. Moran CA, Suster S. Neuroendocrine carcinomas (carcinoid tumor) of the thymus. A clinicopathologic analysis of 80 cases. *Am J Clin Pathol* 2000;114:100–110.
11. Nasu M, Soma T, Fukushima H, et al. Hepatoid carcinoma of the lung with production of alpha-fetoprotein and abnormal prothrombin: an autopsy case report. *Mod Pathol* 1997;10:1054–1058.
12. Morikawa T, Kobayashi S, Yamadori I, et al. Three cases of extrapulmonary small cell carcinoma occurring in the prostate, stomach, and pancreas. *Indian J Cancer* 1994;31:268–273.
13. Yamaguchi T, Imamura Y, Nakayama K, et al. Paranuclear blue inclusions of small cell carcinoma of the stomach: report of a case with cytologic presentation in peritoneal washings. *Acta Cytol* 2005;49:207–212.

Pharmacokinetic Analysis of Carboplatin and Etoposide in a Small Cell Lung Cancer Patient Undergoing Hemodialysis

Ken Takezawa, MD, Isamu Okamoto, MD, PhD, Masahiro Fukuoka, MD, PhD, and Kazuhiko Nakagawa, MD, PhD

Cancer chemotherapy is not well established for patients on hemodialysis (HD). A 77-year-old man on HD presented with small cell lung cancer. He was treated with the combination of carboplatin and etoposide while the pharmacokinetics of the drugs were monitored. The patient showed a response with manageable toxicity and remained progression free for at least 8 months. The area under the concentration-time curve for each antitumor agent in the patient was within the therapeutic range achieved in individuals with normal renal function. Carboplatin and etoposide chemotherapy combined with HD thus allowed the drugs to achieve an appropriate area under the concentration-time curve and sufficient efficacy in a small cell lung cancer patient with chronic renal failure.

Key Words: Small cell lung cancer, Hemodialysis, Pharmacokinetics, Chemotherapy.

(*J Thorac Oncol.* 2008;3: 1073–1075)

The prognosis of patients with chronic renal failure has improved as a result of progress in hemodialysis (HD), and opportunities to treat malignant tumors that develop in such HD patients are increasing. However, little is known of the safety or efficacy of chemotherapy for malignant tumors in HD patients. We analyzed the pharmacokinetics of combination chemotherapy with carboplatin (CBDCA) and etoposide in a patient with small cell lung cancer (SCLC) undergoing HD.

CASE REPORT

A 77-year-old man with chronic renal failure due to diabetic nephropathy presented with a mass in the left hilar area in March 2007. The general condition of the patient, who had undergone HD, three times a week, was fair, with symptoms such as cough, weight loss, and fever being absent. His Eastern Cooperative Oncology Group performance status was 1. Computed tomography of the chest revealed a 45/33 mm mass in the lower left lobe as well as interstitial pneumonia in the lower left and lower right lobes. Histopathologic analysis of a transbronchial biopsy specimen revealed SCLC. No distant metastasis was detected on systemic examinations, and the patient was diagnosed with limited-stage SCLC. Laboratory testing revealed blood urea nitrogen and creatinine levels of 101 and 8.6 mg/dl, respectively. Other examined laboratory parameters were within normal limits, but subsequent evaluation of serum tumor markers revealed an increased level (18.2 ng/ml) of neuron-specific enolase, which is not affected by renal function.[1]

Radiotherapy was not appropriate for the patient because of his bilateral interstitial pneumonia. Given his good performance status and after obtaining informed consent, we treated the patient with the combination of CBDCA and etoposide (Figure 1). On day 1 of the treatment cycle, the patient received an intravenous injection of etoposide (50 mg/m^2) over 60 minutes followed by an intravenous injection of CBDCA (250–275 mg/m^2) also over 60 minutes. HD was initiated 60 minutes after completion of CBDCA administration and was performed for 4 hours. On day 3, etoposide (50 mg/m^2) was administered over 60 minutes and HD was performed for 4 hours beginning 2 hours after completion of etoposide injection. The doses of CBDCA and etoposide as well as the timing of HD were based on previous studies.[2–4] The treatment was well tolerated. Nonhematologic toxicities such as nausea, vomiting, and fatigue were not observed. The patient also did not experience neutoropenia or thrombocytopenia (Nadir neutrophil and platelet counts during 3 cycles of chemotherapy were 2200/μl and 15.5 $\times$ 10^4/μl, respectively). Prophylactic administration of granulocyte colony-stimulating was not carried out. After three cycles of chemotherapy, each separated by an interval of 3 weeks, the tumor had decreased in size and the serum neuron-specific enolase level had decreased to within normal limits (6.3 ng/ml). The patient remained progression free 8 months after the initiation of treatment.

Pharmacokinetic analysis of CBDCA and etoposide was performed for the first and third courses of chemotherapy. Serial blood samples were collected 0, 1, 2, 3, 4, 5, 6, 24, 37, 41, 42, 49, 53, and 54 hours after completion of CBDCA administration as well as 0, 2, 3, 4, 5, 6, 7, 25, 48, 50, 52, 54, 55, and 73 hours after completion of the first etoposide administration. Each blood sample was analyzed for free

Department of Medical Oncology, Kinki University School of Medicine, Osaka, Japan.

Disclosure: The authors declare no conflicts of interest.

Address for correspondence: Isamu Okamoto, MD, PhD, Department of Medical Oncology, Kinki University School of Medicine, 377-2 Ohno-higashi, Osaka-Sayama, Osaka 589-8511, Japan. E-mail: chi-okamoto@dotd.med.kindai.ac.jp

ISSN: 1556-0864/08/0309-1073

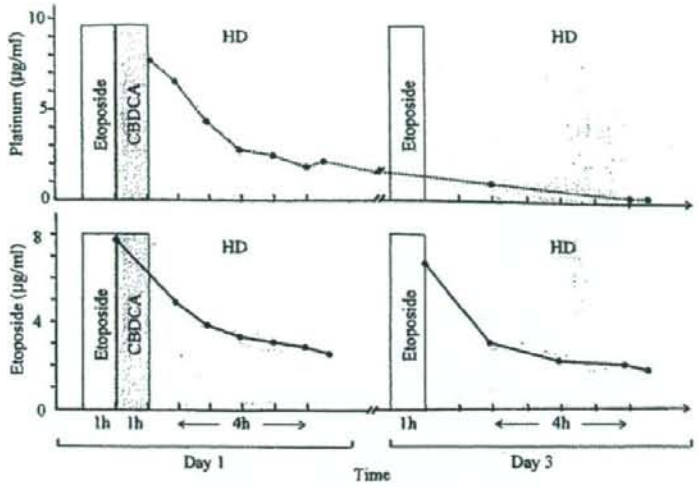

FIGURE 1. Chemotherapy and hemodialysis schedule as well as the plasma concentrations of free platinum and etoposide for the proband. Data are for the first of three cycles of chemotherapy. HD, hemodialysis; CBDCA, carboplatin.

platinum and etoposide (Figure 1) as described previously.[5] In the first cycle, the area under the concentration-time curve (AUC) was 4.10 minutes mg/ml for free platinum and 4401 and 3612 minutes μg/ml for etoposide on days 1 and 3, respectively. In the third course of chemotherapy, for which the CBDCA dose was increased from 250 to 275 mg/m^2, the AUC of free platinum was 4.16 minutes mg/ml. The maximal concentration and half-life of free platinum were 7.7 μg/ml and 2.51 hours in the first cycle and 9.4 μg/ml and 1.93 hours in the third cycle.

DISCUSSION

Many lung cancer patients undergoing HD as a result of impaired renal function may be "undertreated" because chemotherapy regimens are not well established for such individuals. The lack of pharmacokinetic data for most cytotoxic agents in HD patients makes it difficult to administer chemotherapy effectively. Given his old age, bilateral interstitial pneumonia, and renal dysfunction, the present patient might have been considered too high a risk for chemotherapy and recommended to receive best supportive care. However, taking into account the sensitivity of SCLC to platinum combination chemotherapy, we treated him with CBDCA and etoposide while monitoring the pharmacokinetics of these antitumor agents.

CBDCA is a less emetic and less nephrotoxic analog of cisplatin and is preferred over cisplatin for use in patients with renal insufficiency. The desired AUC for CBDCA can be individualized with the use of Calvert's formula on the basis of individual renal function.[6] In previous studies of CBDCA-based chemotherapy in patients undergoing HD, a CBDCA dose of 100 to 150 mg/body was chosen according to this formula, with the glomerular filtration rate set to zero because of the absence of renal function (Table 1).[7–10] In these studies, HD was performed 16 to 24 hours after completion of CBDCA administration, resulting in an AUC of 4.43 to 6.9 minutes mg/ml. More recently, administration of a relatively high dose (300 mg/m^2) of CBDCA with initiation of HD 0.5 to 1.5 hours after completion of drug injection has been shown to be feasible and effective in lung cancer patients undergoing HD.[2–4] However, the AUC of CBDCA in these latter studies was not determined. In the present study, we found that a CBDCA dose of 250 to 275 mg/m^2 administered completely 1 hour before HD gave rise to an AUC for free platinum of 4.10 to 4.16 minutes mg/ml, a therapeutic blood level, consistent with the antitumor efficacy observed

TABLE 1. Previous Studies of Carboplatin-Based Chemotherapy in Cancer Patients on Hemodialysis

	Disease	No. of Patients	Carboplatin Dose	Interval Between Carboplatin Infusion and Hemodialysis (h)	AUC (min mg/ml)
Watanabe et al.[7]	Ovarian cancer	1	125 mg	16	4.43
Jeyabalan et al.[8]	Ovarian cancer	1	125 mg	24	N.D
Chatelut et al.[9]	Ovarian cancer	1	150 mg	24	6.06–6.70
Motzer et al.[10]	Germ cell tumor	2	100 mg/m^2	24	6.7–6.9
Inoue et al.[2]	SCLC	3	300 mg/m^2	1	N.D
Yanagawa et al.[3]	NSCLC/epipharynx ca	2	300 mg/m^2	0.5	N.D
Haraguchi et al.[4]	SCLC	1	300 mg/m^2	1.5	N.D

N.D, not determined; NSCLC, non-small cell lung cancer.

in the previous studies[2–4]. Our presented study supports that relatively high dose administration of CBDCA with initiation of HD 1 hour after drug injection would be an alternative strategy for patients with HD -dependent renal insufficiency.

Etoposide is active against various types of malignant tumors, but its membrane permeability in HD remains unclear. The AUC range for etoposide in 13 patients with normal renal function treated with this drug at a dose of 100 mg/m^2 was previously shown to be 2291 to 6832 minutes μg/ml (Ref. [11]). The present patient was treated with etoposide at 50 mg/m^2 on days 1 and 3, with HD being initiated 2 hours after completion of the drug injection. The AUC of etoposide was 3612 to 4401 minutes μg/ ml, values that are within the range achieved in patients with normal renal function. Indeed, the combination chemotherapy in the proband induced a tumor response that persisted for at least 8 months. Administration of etoposide at 100 mg/m^2 on days 1, 3, and 5 in combination with cisplatin at 80 mg/m^2 was shown to be acceptable in 4 lung cancer patients with renal dysfunction.[12] In the previous study, HD was performed soon after drug administration, resulting in an AUC for etoposide of 4800 to 6204 minutes μg/ml. Data from the previous studies and our present patient thus indicate that etoposide can be administered safely in HD patients.

The present case shows that CBDCA and etoposide chemotherapy combined with HD resulted in AUCs for these drugs within the therapeutic range in a SCLC patient with chronic renal failure. Although further studies are needed, our findings suggest that this regimen of combination chemotherapy can be administered to lung cancer patients with renal insufficiency.

REFERENCES

1. Xiaofang Y, Yue Z, Xialian X, et al. Serum tumour markers in patients with chronic kidney disease. *Scand J Clin Lab Invest* 2007;67:661–667.
2. Inoue A, Saijo Y, Kikuchi T, et al. Pharmacokinetic analysis of combination chemotherapy with carboplatin and etoposide in small-cell lung cancer patients undergoing hemodialysis. *Ann Oncol* 2004;15:51–54.
3. Yanagawa H, Takishita Y, Bando H, et al. Carboplatin-based chemotherapy in patients undergoing hemodialysis. *Anticancer Res* 1996;16: 533–535.
4. Haraguchi N, Satoh H, Ogawa R, et al. Chemotherapy in a patient with small-cell lung cancer undergoing hemodialysis. *Clin Oncol* 2005;17: 663–668.
5. LeRoy AF, Wehling ML, Sponseller HL, et al. Analysis of platinum in biological materials by flameless atomic absorption spectrophotometry. *Biochem Med* 1977;18:184–191.
6. Calvert AH, Newell DR, Gumbrell LA, et al. Carboplatin dosage: prospective evaluation of a simple formula based on renal function. *J Clin Oncol* 1989;7:1748–1756.
7. Watanabe M, Aoki Y, Tomita M, et al. Paclitaxel and carboplatin combination chemotherapy in a hemodialysis patient with advanced ovarian cancer. *Gynecol Oncol* 2002;84:335–338.
8. Jeyabalan N, Hirte HW, Moens F. Treatment of advanced ovarian carcinoma with carboplatin and paclitaxel in a patient with renal failure. *Int J Gynecol Cancer* 2000;10:463–468.
9. Chatelut E, Rostaing L, Gualano V, et al. Pharmacokinetics of carboplatin in a patient suffering from advanced ovarian carcinoma with hemodialysis-dependent renal insufficiency. *Nephron* 1994;66:157–161.
10. Motzer RJ, Niedzwiecki D, Isaacs M, et al. Carboplatin-based chemotherapy with pharmacokinetic analysis for patients with hemodialysis-dependent renal insufficiency. *Cancer Chemother Pharmacol* 1990;27: 234–238.
11. D'Incalci M, Farina P, Sessa C, et al. Pharmacokinetics of VP16–213 given by different administration methods. *Cancer Chemother Pharmacol* 1982;7:141–145.
12. Watanabe R, Takiguchi Y, Moriya T, et al. Feasibility of combination chemotherapy with cisplatin and etoposide for haemodialysis patients with lung cancer. *Br J Cancer* 2003;88:25–30.

Prognostic Significance of Thin-Section CT Scan Findings in Small-Sized Lung Adenocarcinoma*

Toshihiko Hashizume, MD; Kouzo Yamada, MD; Naoyuki Okamoto, PhD; Haruhiro Saito, MD; Fumihiro Oshita, MD; Yasufumi Kato, MD; Hiroyuki Ito, MD; Haruhiko Nakayama, MD; Youichi Kameda, MD; and Kazumasa Noda, MD

Objectives: **The purpose of this study is to evaluate the prognostic importance of thin-section (TS) CT scan findings in small-sized lung adenocarcinomas.**

Patients and methods: **We reviewed TS-CT scan findings and pathologic specimens from 359 consecutive patients who underwent surgical resection for peripheral lung adenocarcinomas ≤ 20 mm in diameter during the period from July 1997 to May 2006. By using TS-CT scan images, tumors were defined as air-containing types if the maximum diameter of tumor opacity on mediastinal window images was less than or equal to half of that seen on lung window images, and as a solid-density type if the maximum diameter on the mediastinal window images was more than half of that on lung window images. We compared TS-CT scan findings to pathologic findings (*ie*, lymph node metastasis, pleural invasion, vessel invasion, and lymphatic invasion) and prognosis. The following prognostic factors were analyzed by χ^2 test and Cox proportional hazard model: age; gender; tumor size; pathologic stage; TS-CT scan findings; histologic subtypes defined by Noguchi et al (*ie*, Noguchi type); pleural involvement; lymphatic invasion; and vascular invasion.**

Results: **No pathologic invasive findings or recurrence were found in patients with air-containing-type tumors. Pathologic invasive findings and recurrence were found in 10 to 30% of patients with solid-density-type tumors. The air-containing type tumors seen on TS-CT scans and Noguchi type A or B tumors were demonstrated as prognostic factors for good outcome by χ^2 test ($p < 0.001$). Multivariate analyses revealed lymphatic permeation as a significant prognostic factor.**

Conclusion: **The TS-CT scan findings were important predictive factors for postsurgical outcome in patients with lung adenocarcinoma.** ***(CHEST 2008; 133:441–447)***

Key words: bronchioloalveolar cell carcinoma; ground-glass opacity; limited surgery; noninvasive cancer

Abbreviations: BAC = bronchioloalveolar cell carcinoma; GGO = ground-glass opacity; HU = Hounsfield units; TS = thin section

The number of patients with small-sized lung carcinoma has been increasing due to the routine clinical use of CT scanning and the increasing use of helical CT scan screening for lung cancer. Adenocarcinoma is the most common histologic type of lung cancer in those cases. The population of lung adenocarcinoma is heterogeneous, and many subtypes of adenocarcinoma have been advocated.[1,2] For example, Noguchi et al[1] classified small-sized lung adenocarcinoma into six subtypes based on tumor growth patterns. In this study, a type A or B tumor was localized bronchioloalveolar cell carcinoma (BAC), which showed no lymph node metastasis, rare vascular and pleural invasion, and excellent prognosis (5-year survival rate, 100%). A type C tumor was BAC with foci of active fibroblast proliferation, and showed pathologic invasive findings, and poor prognosis (5-year survival rate, 74.8%). A type D, E, or F tumor was adenocarcinoma without BAC and showed worst prognosis (5-year survival rate, 52.4%). Although these pathologic characteristics are useful as prognostic indicators, the results are defined only after surgery. If we have techniques by which we know the biological behavior of the tumor

and prognosis before treatment, they may be useful for planning therapy.

Many investigators reported that preoperative CT scan findings were related to the pathologic features and prognosis after resection of the tumor. The ratio of ground-glass opacity (GGO), defined as a hazy increase in lung attenuation without obscuring the underlying vascular marking on the CT scan, was associated with the histologic type of the tumor and survival. One of the purposes of these studies was to determine noninvasive carcinoma, defined as a tumor without lymph node metastasis, pleural invasion, vascular invasion, and lymphatic invasion by using thin-section (TS) CT scan images. However, there are few articles accurately determining noninvasive carcinoma by TS-CT scan images. If we determine a diagnosis of noninvasive carcinoma using CT scan images, they are useful for deciding on the surgical procedure to be used, especially lesser resection. This study was carried out to determine whether TS-CT scan findings were good indicators of noninvasive carcinoma of the lung, and also to clarify whether TS-CT scan findings were related to the prognosis.

Materials and Methods

We reviewed TS-CT scan findings and pathologic specimens from 359 consecutive patients who underwent surgical resection for peripheral adenocarcinomas ≤ 20 mm in diameter during the period from July 1997 to May 2006. All patients underwent physical examination, chest roentgenography, CT scan of the chest and abdomen, bone scintigraphy, and MRI of the brain for the staging and evaluation of resectability before the operation. The patients with disease of clinical stage IIB or less underwent surgery. We also surgically treated the patients with clinical N2 disease without evidence of mediastinal lymph node metastasis proven by mediastinoscopy. This study was approved by our institutional review board after confirmation of informed consent by the patients for us to review their records and images. Chest CT scan images were obtained by a commercially available scanner (X-Vigor/Real or Aquilion M/16 CT scanner; Toshiba Medical Systems; Tokyo, Japan). Conventional CT scan images were obtained serially from the thoracic inlet to the lung bases at 120 kV peak spacing, 512 × 512 pixel resolution, and 1-s scanning time. TS images targeted to the tumor were obtained serially at 120 kVp and 200 mA, with 2-mm section thickness, pitch 1, section spacing of 1 to 2 mm, 512 × 512 pixel resolution, and 1-s scanning time, using a high-spatial-reconstruction algorithm with a 20-cm field of view. These images were printed as photographs on each sheet of films using a mediastinal window level setting (level, 40 Hounsfield units [HU]; width, 400 HU) and a pulmonary window level setting (level, −600 HU; width, 1,600 HU).

While contrast medium (60 mL) was infused IV during imaging, lesion sites were translocated in a helical scan mode with a CT scan table speed of 2 mm/s; TS-CT scan images were obtained at one breath hold (120 kVp; 200 mA). The time interval between CT scan examination and subsequent surgery was ≤ 2 weeks in all patients. All CT scan images were reviewed by four thoracic oncologists who were not informed of the pathologic findings. They obtained the maximum dimension of the tumor using a pulmonary window level setting and the maximum dimension of the tumor using a mediastinal window level setting from the TS-CT scan images.

Tumors were defined as air-containing types if the ratio of the maximum dimension of the tumor using a mediastinal window level setting to the maximum dimension of the tumor using a pulmonary window level setting was ≤ 50%, and were defined as solid-density types if it was > 50%. Examples of CT scan images of the two groups are shown in Figures 1 and 2.

Each pattern based on TS-CT scan images was evaluated in terms of pathologic findings and survival outcome. We evaluated pathologic stage (TNM system), pleural involvement, vascular invasion, and lymphatic invasion. In addition, pathologic subtypes defined by Noguchi et al[1] (called hereafter *Noguchi type*) were evaluated.

The statistical significance of the difference between the incidence of relapse and TS-CT scan findings or Noguchi type was assessed by χ^2 tests. Relapse-free survival was calculated by the Kaplan-Meier method. Log-rank tests were used to compare the Kaplan-Meier curves. The Cox proportional hazards model was applied for multivariate analysis. Significance was defined as $p < 0.05$.

Results

Patient and tumor characteristics are listed in Table 1. There were 60 cases in which the largest diameter of the lesion was ≤ 10 mm, 130 cases in which it was 11 to 15 mm, and 169 cases in which it was 16 to 20 mm. There were 152 patients with air-containing-type tumors, and 207 patients with solid-density-type tumors. Table 2 shows the relationship between TS-CT scan findings and pathologic findings. No patients with air-containing-type tumors had lymph node metastasis, pleural involvement, vascular invasion, or lymphatic permeation. Among patients with solid-density-type tumors, 23 (11%) had lymph node metastasis, 45 (22%) had pleural involvement, 69 (33%) had vascular invasion, and 41 (20%) had lymphatic permeation. Table 3 shows the relationship between TS-CT scan findings and

*From the Department of Respiratory Medicine (Dr. Hashizume), Yamato City Hospital, Kanagawa, Japan; and the Departments of Thoracic Oncology (Drs. Yamada, Saito, Oshita, and Noda), Thoracic Surgery (Drs Kato, Ito, and Nakayama), Research Institute (Dr. Okamoto), and Pathology (Dr. Kameda), Kanagawa Cancer Center, Yokohama, Japan.
This work was supported in part by a grant for Scientific Research Expenses for Health Labour and Welfare Programs, and by the Foundation for the Promotion of Cancer Research and the Second-Term Comprehensive 10-year Strategy for Cancer Control.
The authors have reported to the ACCP that no significant conflicts of interest exist with any companies/organizations whose products or services may be discussed in this article.
Manuscript received August 6, 2007; revision accepted October 29, 2007.

Correspondence to: Toshihiko Hashizume, MD, Yamato City Hospital, Department of Respiratory Medicine, Fukami-nishi 8-3-6, Yamato-city, Kanagawa, 242-8602 Japan; e-mail: toshi@yk9.so-net.ne.jp
DOI: 10.1378/chest.07-1533

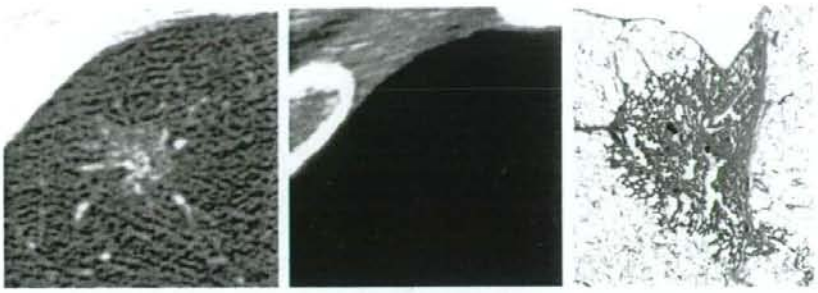

FIGURE 1. TS-CT scan findings of an air-containing-type tumor (diameter, 13 mm) on lung window setting images (*left*, *a*) and on mediastinal window setting images (*center*, *b*). The histologic specimen (*right*, *c*) shows BAC (hematoxylin-eosin, original × 6).

pathologic stage. All patients with air-containing-type tumors had pathologic stage IA disease. In contrast, 39 patients (19%) with solid-density-type tumors had pathologic stage IB or greater disease. Table 5 shows the relationship between TS-CT scan findings and Noguchi type tumors. Among 152 patients with air-containing-type tumors, 79 patients received lobectomy, while 73 underwent limited resections (*ie*, segmentectomy or wedge resection) because of their small size (median tumor diameter, 11 mm). Among 207 patients with solid-density-type tumors, 3 patients underwent pneumonectomy and 155 underwent lobectomy, while 49 underwent limited resections because of their being elderly or having pulmonary hypofunction.

Table 2 shows the relationship between TS-CT scan findings and cancer relapse after surgery. No postoperative cancer relapse was seen in patients with air-containing-type tumors; in contrast, relapse was found in 31 patients (15%) with solid-density-type tumors. The relapse-free survival of 207 patients for whom ≥ 3 years have passed since surgery is shown in Figure 3. Patients with air-containing-type tumors had a 100% 5-year relapse-free survival rate, which was significantly better than that for patients with solid-density-type tumors ($p < 0.001$).

We assessed prognostic factors in 207 patients for whom ≥ 3 years had passed since undergoing surgery. Table 5 shows the relationship between cancer relapse and TS-CT scan findings or Noguchi type. No cancer relapse was seen patients with air-containing-type tumors or patients with Noguchi type A or B tumors. The presence of both air-containing-type and Noguchi type A or B tumors were demonstrated as significant prognostic factors for good outcome by χ^2 tests ($p < 0.001$). The reason for using χ^2 tests but not Cox proportional hazards models to analyze the prognostic factors for TS-CT scan findings and Noguchi type tumors was due to the difficulty in conducting a statistical analysis at the time of no relapse event in the patient group with air-containing-type tumors or Noguchi type A or B tumors. Then, a multivariate analysis with a Cox pro-

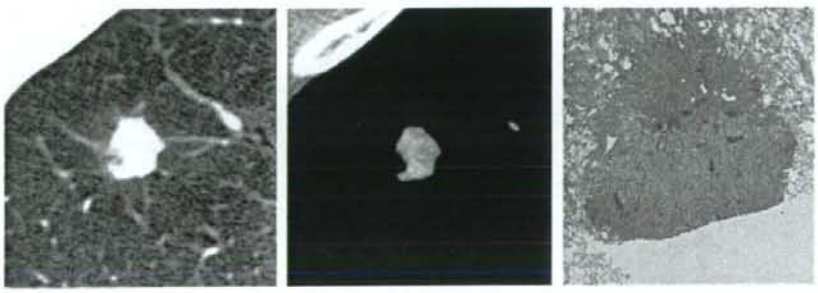

FIGURE 2. TS-CT scan findings for a solid-density-type tumor (diameter, 14 mm) on lung window setting images (*left*, *a*) and on mediastinal window setting images (*center*, *b*). The histologic specimen (*right*, *c*) shows poorly differentiated adenocarcinoma (hematoxylin-eosin, original × 6).

Table 1—*Patient and Tumor Characteristics

Variables	Values
Patients, No.	359
Age, yr	29–86 (65)
Gender, No.	
Male	159
Female	200
Tumor size, mm	5–20 (15)
Noguchi type tumor, No.	
Type A	52
Type B	75
Type C	162
Type D	39
Type E	5
Type F	25
TS-CT scan findings, No.	
Air-containing-type tumor	152
Solid-density-type tumor	207

*Values are given as range (median) or No.

portional hazard model was performed in 116 patients without air-containing type tumors or Noguchi type A or B tumors. The results showed that lymphatic permeation was a significant prognostic factor (Table 6).

Discussion

In patients with small-sized lung adenocarcinomas, several authors[1,2] have shown that pathologic characteristics are correlated with prognosis. Noguchi et al[1] have used tumor growth patterns to classify small-sized adenocarcinomas into six subtypes (*ie*, types A to F). Small, localized BACs (*ie*, types A and B) have not yet metastasized to lymph nodes or invaded vessels or pleura, and are associated with an excellent prognosis (5-year survival rate, 100%). Localized BAC with central fibrosis formation (*ie*, type C) is thought to be advanced carcinoma, which progresses from type A or B and is associated with a poorer prognosis than before (5-year survival rate, 74.8%). The prognosis for patients with nonreplacement-type adenocarcinomas (*ie*, types D, E, or F) is worse than that for patients with replacement-type adenocarcinomas (*ie*, types A, B, and C) [5-year survival rate, 52.4%]. Suzuki et al[3] showed that the size of the central fibrosis was a prognostic factor among peripheral lung adenocarcinomas that were ≤ 3.0 cm in size. In this study, the patients with adenocarcinoma having central fibrosis ≤ 5 mm in the maximum dimension had a 5-year survival rate of 100%, whereas the other patients had a 5-year survival rate of 70%. Higashiyama et al[4] showed that the component area of BAC was correlated with postoperative survival in patients with small peripheral adenocarcinomas ≤ 2.0 cm in diameter. Patients with adenocarcinoma having a BAC component comprising < 50% of the tumor tissue showed a significantly poorer prognosis than those with ≥ 50%.

In TS-CT scan images, consolidation areas represent mostly the foci of fibrosis or tumors of a solid growth pattern, whereas GGO areas reflect areas of a growth pattern of tumor cells replacing alveolar lining cells such as BAC. Because the fibrotic foci increase with the progression of the tumor, and because these areas and advanced adenocarcinomas with a solid growth pattern demonstrate consolidation areas on CT scans, it is suggested that the percentage of the consolidation or GGO areas relative to the tumor is a prognostic indicator. Many investigators[5–22] have reported on the correlation among TS-CT scan findings, pathologic findings, and prognosis. These studies have shown that GGO ratios were very much associated with BAC ratios and had favorable prognostic factors. However, the methods used to calculate the percentage of GGO areas (*ie*, GGO ratio) differ in different articles. Besides, we have few articles that have accurately determined the presence of noninvasive carcinoma, which was defined as a tumor without lymph node

Table 2—*Relationship Between TS-CT Findings and Both Pathologic Findings and Recurrence*

	TS-CT Scan Findings	
Pathologic Findings	Air-Containing-Type Tumors (n = 152)	Solid-Density-Type Tumors (n = 207)
Lymph node metastasis	0	23
Pleural involvement	0	45
Lymphatic permeation	0	41
Vascular invasion	0	69
Recurrence	0	31

Table 3—*Relationship Between TS-CT Findings and Pathologic Stage*

	Pathologic Stage					
TS-CT Scan Findings	IA	IB	IIA	IIB	IIIA	IIIB
Air-containing-type tumor	152	0	0	0	0	0
Solid-density-type tumor	167	16	5	3	15	1

Table 4—*Relationship Between TS-CT Findings and Noguchi Type*

	Noguchi Type					
TS-CT Scan Findings	A	B	C	D	E	F
Air-containing-type tumor	49	53	49	0	0	1
Solid-density-type tumor	3	22	113	39	5	24

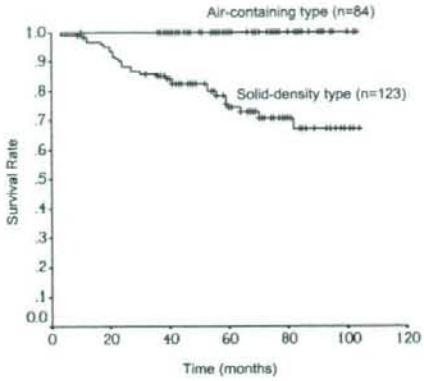

FIGURE 3. Relapse-free survival curves in patients with air-containing-type tumors and solid-density-type tumors.

metastasis, pleural invasion, vascular invasion, and lymphatic invasion, by TS-CT scan images. The parameters used to calculate the GGO ratio that have previously been reported are as follows: a GGO/tumor area ratio[5–10]; a consolidation/tumor dimension ratio[11–14]; a GGO/tumor volume ratio[15]; an area ratio of tumor on mediastinal window to that on the lung window[16,17]; a product of the dimension ratio of the tumor on the mediastinal window to that on lung window[18–20]; and a maximum dimension of tumor on the mediastinal window.[21] Matsuguma et al[8] reported on the relation between the proportion of the GGO and both clinicopathologic characteristics and tumor recurrence in patients with clinical T1N0M0 adenocarcinoma. In this study, the patients with a GGO ratio of ≥ 50% seen on high-resolution CT scans had neither lymph node metastasis nor lymphatic invasion and were alive without cancer recurrence. Ohde et al[12] reported the relation between the proportion of consolidation to GGO and pathologic invasive findings in patients with lung adenocarcinomas ≤ 3.0 cm. They showed that all tumors in which the ratio of the greatest diameter of consolidation to that of the tumor was ≤ 50% had neither lymph node metastasis nor vessel invasion and 5-year survival rate of 95.7%. Although only one cancer relapse was seen in tumors with a ratio of the greatest diameter of consolidation to that of the tumor of ≤ 50% in the study by Ohde et al[12]; the methods used to calculate the GGO ratio in these two studies[8,12] may be useful in defining noninvasive cancer. On the other hand, several investigators[16–20] used not only lung window images but also mediastinal window images to classify the tumors on TS-CT scan images. Kondo et al[16] used a ratio of the tumor area on the mediastinal window images to that on lung window images in patients with pulmonary adenocarcinoma of ≤ 2.0 cm, and showed that the tumors with a ratio of ≤ 50% had no lymph node metastasis, rare vascular invasion, and no cancer relapse. Okada et al[18] and Shimizu et al[20] used the tumor shadow disappearance rate, which was determined from the product of the maximum dimension of the tumor and the largest dimension perpendicular to the maximum axis on both pulmonary and mediastinal window images on TS-CT scan, as previously described by Takamochi et al.[22] They showed that the tumors with a tumor shadow disappearance rate of ≥ 50% had no lymph node metastasis, rare vascular invasion, and no cancer relapse in patients with lung adenocarcinomas ≤ 2.0 cm in diameter. However, the methods used to classify the tumors in these studies with both pulmonary and mediastinal window images could not completely discriminate the tumor without invasive findings (*ie*, vascular, lymphatic, and pleural involvement) from the other. In contrast, the present study showed that the air-containing-type tumor did not have lymph node metastasis, pleural involvement, vessel invasion, or lymphatic permeation, and did not recur after resection. These results suggest that the air-containing-type tumor should be defined as a noninvasive cancer.

The GGO area is sometimes neither clear nor objective. We sometimes experienced cases in which the border of consolidation and the GGO shadow on the TS-CT scan was unclear, and it was difficult or impossible to measure this size accurately. To select noninvasive cancer more simply and more objectively, we measured the maximum dimensions of tumors on both the lung and mediastinal windows. Our classification has the advantage of simplicity and objectiveness. We have only to compare the greatest dimension of the tumor on lung window images with that on mediastinal images of the TS-CT scan.

Although a number of prognostic indicators have been proposed such as TNM staging, tumor differentiation, molecular expression, and vascular inva-

Table 5—*Relationship Between Recurrence and Both TS-CT Findings and Noguchi Type Tumor in 207 Patients for Whom 3 Years or More Have Passed Since Surgery*

TS-CT Scan Findings	Recurrence		p Value
	No	Yes	
Tumors			0.000
Air-containing type	84	0	
Solid-density type	93	30	
Noguchi type tumor			0.000
Type A or B	66	0	
Type C, D, E, or F	111	30	

Table 6—*Multivariate Analysis of Relapse-Free Survival*

Variables	Hazard Ratio	95% Confidence Interval	p Value
Age	0.968	0.923–1.014	0.170
Gender (male vs female)	2.372	0.986–5.707	0.054
Tumor size	1.062	0.947–1.192	0.305
Pathologic stage (≥ II vs I)	1.795	0.598–5.389	0.297
Noguchi type tumor (type D, E, or F vs type C)	2.169	0.842–5.586	0.109
Pleural involvement (positive vs negative)	2.181	0.951–5.001	0.066
Lymphatic permeation (positive vs negative)	2.819	1.094–7.265	0.032
Vascular invasion (positive vs negative)	0.864	0.289–2.588	0.795
Operation mode (lobectomy vs wedge resection)	0.453	0.188–1.094	0.079

sion, the final results are defined only after surgery. As yet, no definite preoperative indicators have been discovered for the postoperative outcome of patients with adenocarcinomas. This study showed that preoperative TS-CT scan findings had prognostic importance. The air-containing-type tumor defined in this study showed no cancer relapse and was revealed as an independent prognostic factor for relapse-free survival. The identification of prognostic variables, especially before the operation is important to decide on the operative procedure and adjuvant therapy. Although lobectomy and pneumonectomy with systemic mediastinal lymphadenectomy is the standard surgical treatment for non-small cell lung cancer, if noninvasive lung cancers are distinguishable on CT scans, limited surgery can be indicated before the operation. Since patients with the air-containing-type tumor showed neither pathologic invasion nor relapse after surgery, we think it is reasonable that we can treat patients with lesser resection for tumors of this type. Treating patients with limited resection leads to a reduction in operative complications and the maintenance of pulmonary function. The number of both elderly patients with lung cancer and patients with a second lung cancer has been increasing. Lesser invasive techniques such as limited resection and stereotactic radiotherapy will play an important role in the future. Studies[23,24] have shown the results of the attempt to apply limited surgery for small lung tumors ≤ 2.0 cm in diameter, in which a small number of local relapses was seen in patients who underwent limited resections. Our study also showed that 11% of solid-density-type tumors had lymph node metastasis. We think that it is not the size of the tumor but the findings of the CT scan of the tumor that is a good indicator for determining whether to use limited resection. Nakata et al[25] reported the results of limited resection of pure GGO selected by the CT scan, in which no cancer relapse was seen in 33 patients who underwent limited resection. In the selection of a candidate for limited surgery, it is important to select patients with noninvasive cancers that not only have high specificity but also high sensitivity. In our study, among 162 patients with Noguchi type C tumor, which is thought to be advanced carcinoma, 49 patients had air-containing-type tumors (Table 4). This result means that our classification using TS-CT scans can preoperatively determine the presence of type C tumors without invasive findings. A prospective study is needed to clarify whether patients with air-containing-type tumors defined preoperatively on TS-CT scan images are candidates for limited surgery. In conclusion, the presence of air-containing-type tumors in patients with peripheral adenocarcinomas < 2.0 cm in diameter means noninvasive cancer and that such patients are candidates for limited surgery.

References

1 Noguchi M, Morikawa A, Kawasaki M, et al. Small adenocarcinoma of the lung: histologic characteristics and prognosis. Cancer 1995; 75:2844–2852

2 Kurokawa T, Matsuno Y, Noguchi M, et al. Surgically curable "early" adenocarcinoma in the periphery of the lung. Am J Surg Pathol 1994; 18:431–438

3 Suzuki K, Yokose T, Yoshida J, et al. Prognostic significance of the size of central fibrosis in peripheral adenocarcinoma of the lung. Ann Thorac Surg 2000; 69:893–897

4 Higashiyama M, Kodama K, Yokouchi H, et al. Prognostic value of bronchiolo-alveolar carcinoma component of small lung adenocarcinoma, Ann Thorac Surg 1999; 68:2069–2073

5 Kuriyama K, Seto M, Kasugai T, et al. Ground-glass opacity on thin-section CT: value in differentiating subtypes of adenocarcinoma of the lung. AJR Am J Roentgenol 1999; 173:465–469

6 Kodama K, Higashiyama M, Yokouchi H, et al. Prognostic value of ground-glass opacity found in small lung adenocarcinoma on high-resolution CT scanning. Lung Cancer 2001; 33:17–25

7 Kim E, Johkoh T, Lee KS, et al. Quantification of ground-glass opacity on high-resolution CT of small peripheral adenocarcinoma of the lung: pathologic and prognostic implications. AJR Am J Roentgenol 2001; 177:1417–1422

8 Matsuguma H, Yokoi K, Anraku M, et al. Proportion of ground-glass opacity on high-resolution computed tomography in clinical T1N0M0 adenocarcinoma of the lung: a predictor of lymph node metastasis. J Thorac Cardiovasc Surg 2002; 124:278–284

9 Takashima S, Maruyama Y, Hasegawa M, et al. Prognostic significance of high-resolution CT findings in small peripheral adenocarcinoma of the lung: a retrospective study on 64 patients. Lung Cancer 2002; 36:289–295

10 Matsuguma H, Nakahara R, Anraku M, et al. Objective definition and measurement method of ground-glass opacity for planning limited resection in patients with clinical stage IA

adenocarcinoma of the lung. Eur J Cardiothorac Surg 2004; 25:1102–1106
11 Aoki T, Tomoda Y, Watanabe H, et al. Peripheral lung adenocarcinoma: correlation of thin-section CT findings with histologic prognostic factors and survival. Radiology 2001; 220:803–809
12 Ohde Y, Nagai K, Yoshida J, et al. The proportion of consolidation to ground-glass opacity on high resolution CT is a good predictor for distinguishing the population of non-invasive peripheral adenocarcinoma. Lung Cancer 2003; 42: 303–310
13 Sakao Y, Nakazono T, Sakuragi T, et al. Predictive factors for survival in surgically resected clinical IA peripheral adenocarcinoma of the lung. Ann Thorac Surg 2004; 77:1157–1162
14 Ikeda N, Maeda J, Yashima K, et al. A clinicopathological study of resected adenocarcinoma 2 cm or less in diameter. Ann Thorac Surg 2004; 78:1011–1016
15 Tateishi U, Uno H, Yonemori K, et al. Prediction of lung adenocarcinoma without vessel invasion: a CT scan volumetric analysis. Chest 2005; 128:3276–3283
16 Kondo T, Yamada K, Noda K, et al. Radiologic-prognostic correlation in patients with small pulmonary adenocarcinomas. Lung Cancer 2002; 36:49–57
17 Dong B, Sato M, Sagawa M, et al. Computed tomographic image comparison between mediastinal and lung windows provides possible prognostic information in patients with small peripheral lung adenocarcinoma. J Thorac Cardiovasc Surg 2002; 124:1014–1020
18 Okada M, Nishio W, Sakamoto T, et al. Discrepancy of computed tomographic image between lung and mediastinal windows as a prognostic implication in small lung adenocarcinoma. Ann Thorac Surg 2003; 76:1828–1832
19 Takamochi K, Yoshida J, Nishimura M, et al. Prognosis and histologic features of small pulmonary adenocarcinoma based on serum carcinoembryonic antigen level and computed tomographic findings. Eur J Cardiothorac Surg 2004; 25:877–883
20 Shimizu K, Yamada K, Saito H, et al. Surgically curable peripheral lung carcinoma: correlation of thin-section CT findings with histologic prognostic factors and survival. Chest 2005; 127:871–878
21 Sakao Y, Nakazono T, Tomimitsu S, et al. Lung adenocarcinoma can be subtyped according to tumor dimension by computed tomography mediastinal-window setting: additional size criteria for clinical T1 adenocarcinoma. Eur J Cardiothorac Surg 2004; 26:1211–1215
22 Takamochi K, Nagai K, Yoshida J, et al. Pathologic N0 status in pulmonary adenocarcinoma is predictable by comparing serum carcinoembryonic antigen level and computed tomographic findings. J Thorac Cardiovasc Surg 2001; 122:325–330
23 Kodama K, Doi O, Higashiyama M, et al. Intentional limited resection for selected patients with T1N0M0 non-small-cell lung cancer: a single-institution study. J Thorac Cardiovasc Surg 1997; 114:347–353
24 Tsubota N, Ayabe K, Doi O, et al. Ongoing prospective study of segmentectomy for small lung tumors. Ann Thorac Surg 1998; 66:1787–1790
25 Nakata M, Sawada S, Saeki H, et al. Prospective study of thoracoscopic limited resection for ground-glass opacity selected by computed tomography. Ann Thorac Surg 2003; 75:1601–1606

EXPERT REVIEWS

Gefitinib for the treatment of non-small-cell lung cancer

Expert Rev. Anticancer Ther. 9(1), 17–35 (2009)

Toyoaki Hida†, Shizu Ogawa, Jang Chul Park, Ji Young Park, Junichi Shimizu, Yoshitsugu Horio and Kimihide Yoshida

†Author for correspondence
Department of Thoracic Oncology, Aichi Cancer Center Hospital, 1-1 Kanokoden, Chikusa-ku, Nagoya 464-8681, Japan
Tel.: +81 527 626 111
Fax: +81 527 642 963
107974@aichi-cc.jp

Gefitinib is an orally bioavailable, EGF receptor tyrosine kinase inhibitor and was the first targeted drug to be approved for non-small-cell lung cancer (NSCLC). Identification of objective tumor regressions with gefitinib in NSCLC patients has resulted in intense, worldwide clinical and basic research directed toward finding the optimal use of gefitinib in NSCLC. A recent large international Phase III study (IRESSA NSCLC Trial Evaluating Response and Survival Against Taxotere [INTEREST]) comparing gefitinib and docetaxel in unselected pretreated patients showed equivalent survival with better tolerability and quality of life. In addition, a Phase III study (WJTOG0203) evaluating gefitinib as sequential therapy after platinum-doublet chemotherapy showed the improved progression-free survival time. Furthermore, a large-scale randomized study (IRESSA Pan-Asia study [IPASS]) comparing gefitinib monotherapy with carboplatin/paclitaxel for previously untreated patients with adenocarcinoma who were never- or light-smokers showed an improved progression-free survival time in the gefitinib arm. A smaller Phase III study of pretreated Japanese patients (V-15-32) also demonstrated no difference in overall survival compared with docetaxel, with a statistically greater overall response rate. Somatic mutations in the *EGFR* gene, the target of gefitinib, were associated with dramatic and durable regressions in patients with NSCLC. Currently, investigators are trying to determine the optimal approach to select patients for treatment with gefitinib. This article aims to briefly summarize the profile of gefitinib, *EGFR* mutations, landmark trials with gefitinib and, also, ongoing trials that may herald an era of individualized therapy in at least some NSCLC patients.

KEYWORDS: EGF receptor • *EGFR* gene mutation • gefitinib • non-small-cell lung cancer • tyrosine kinase inhibitor

Lung cancer is the most common cause of cancer deaths worldwide. Lung cancer is divided into two morphological types: small-cell lung cancer (SCLC) and non-small-cell lung cancer (NSCLC). SCLC is a distinct clinicopathological entity with a highly aggressive clinical course and neuroendocrine properties. Patients with SCLC are generally more sensitive to a variety of cytotoxic drugs and radiation therapy compared with NSCLC patients. NSCLC, which is less sensitive to chemotherapeutic agents, accounts for over 80% of all lung cancers and NSCLC can be further subdivided by histological type into adenocarcinoma, squamous-cell carcinoma, large-cell carcinoma and others. Adenocarcinoma is the predominant histological subtype and is increasing among patients with lung cancer. Among adenocarcinoma bronchioloalveolar carcinoma is a well-differentiated subtype originating in the peripheral lung that spreads through the airways.

Currently, platinum-based combination chemotherapy regimens, including several active new chemotherapeutic agents, comprise the standard option for patients with advanced NSCLC and good performance status. However, various combinations of drugs have similar efficacy, producing objective response rates of 30–40%, a median survival time of 8–10 months and 1-year survival rates of 30–40% [1–3]. These results remain unsatisfactory and new modalities of treatment are urgently awaited. Recently, novel molecular-targeted strategies that block cancer progression pathways have been suggested as a more cancer cell-specific treatment to control cancer and are considered an exciting therapeutic approach for treating NSCLC [4]. The development of agents that target the EGF receptor (EGFR) signal transduction pathways have provided a class of novel targeted therapeutic agents with improved side-effect profiles compared with conventional chemotherapeutic agents. EGFR is a promising target for anticancer therapy because it is expressed in a variety of tumors, including NSCLC [5]. Furthermore, high levels of EGFR expression have been associated with a poor prognosis in lung cancer patients in several studies.

 10.1586/14737140.9.1.17 ISSN 1473-7140

EGFR-targeted cancer therapies are being developed currently, and gefitinib (IRESSA®; AstraZeneca, Wilmington, DE, USA) is an orally active, selective EGFR tyrosine kinase inhibitor (TKI) that blocks signal transduction pathways implicated in the proliferation and survival of cancer cells.

Overview of the market

Lung cancer frequently presents at an advanced and biologically aggressive stage, resulting in poor prognosis. Surgery, chemotherapy and radiation have been generally unsatisfactory, especially in the treatment of advanced disease, and new strategies based on better understanding of the biology are clearly needed to improve the treatment efficacy of this fatal disease. The development of agents that target EGFR signal transduction pathways have provided a class of novel targeted therapeutic agents. Different approaches to inhibiting EGFR have resulted in a number of EGFR-targeted agents in clinical development, including small-molecule EGFR TKIs and monoclonal antibodies. The role of cetuximab (Erbitux®), a monoclonal antibody directed at the extracellular domain of the EGFR, and of gefitinib and erlotinib (Tarceva®; OSI Pharmaceuticals, NY, USA), oral, low-molecular-weight ATP-competitive inhibitors of the EGFR's tyrosine kinase domain is under investigation. Anti-EGFR monoclonal antibodies have demonstrated activity in the therapy of advanced colorectal carcinoma [6] and in a variety of epithelial tumor types, including head and neck cancer and NSCLC. A large Phase III study has found that targeted therapy with cetuximab, combined with platinum-based chemotherapy, improves survival outcome as a first-line treatment for patients with advanced NSCLC (overall survival [OS]: 11.3 months vs 10.1 months; p = 0.044) [7]. Erlotinib is another TKI with slightly different pharmacologic characteristics from gefitinib. Similar to gefitinib, erlotinib is a potent inhibitor of EGFR autophosphorylation, with a concentration that inhibits 50% in the nanomolar range *in vitro*. Erlotinib is the only EGFR TKI approved based on demonstrating improved survival versus placebo, which was observed in patients with advanced NSCLC who had been treated previously with chemotherapy. The randomized study (BR.21 study) brought erlotinib to registration by the US FDA on November 19, 2004, for the treatment of second- and third-line advanced NSCLC [8]. Other EGFR TKIs are currently under investigation in Phase I/II trials, many of which have differing selectivities for the various members of the human EGFR family. In the near future, gefitinib and erlotinib may face competition from EGFR-specific TKIs, such as EKB-569 (Wyeth, Maidenhead, UK) and CL-387785 (Calbiochem, CA, USA), and EGFR-family TKIs, such as BIBW-2992 (Boehringer Ingelheim, Berkshire, UK), HKI-272 (Wyeth), PKI-166 (Novartis), GW-572016 (GlaxoSmithKline, NC, USA), CI-1033 (Pfizer, MI, USA) and PF-00299804 (Pfizer). The VEGF pathway forms another target for cancer treatment, because the growth of solid tumor is angiogenesis dependent. VEGF and EGF exert their biological effects directly or indirectly on tumor growth and metastasis/invasion, as well as on tumor angiogenesis. The biological effects by VEGF and EGF are mediated through activation of their specific downstream signaling, but both factors also share common downstream signaling pathways. There is, thus, the potential for improved therapeutic efficacy by the combination of both EGF/EGFR-targeting and VEGF/VEGF receptor-targeting drugs, although they have a different side-effect profile. It may also face competition later on from multitargeted TKIs, such as ZD6474 (AstraZeneca), AEE-788 (Novartis) and XL647 (Exelixis Inc., San Francisco, CA, USA). Karaman *et al.* have reported small-molecule kinase interaction maps, which provide a useful graphic overview of how compounds interact with the kinome [9].

Gefitinib: an EGFR TKI

Gefitinib is the first molecularly targeted agent to be registered for advanced NSCLC. In Phase II clinical trials, the selective and orally active EGFR TKI gefitinib produced objective tumor responses and symptom improvement in patients with NSCLC who had previously received chemotherapy (response rates of 12–18% and symptom improvement rates of 40–44% in IRESSA Dose Evaluation in Advanced Lung Cancer [IDEAL]-1 and -2) [10,11]. Partial clinical responses to gefitinib have been observed most frequently in women, never-smokers and patients with adenocarcinomas. The IRESSA Survival Evaluation in Lung Cancer (ISEL) study also showed a survival benefit for gefitinib over placebo in Asian patients and never-smokers [12]. Thus, gefitinib clinical trials have shown that higher response rates and longer survival are associated with specific patient characteristics. Using conventional doublet chemotherapy simultaneously with gefitinib or erlotinib in unselected first-line patients does not increase survival [13–16], but the results of a recent Phase III study showed that gefitinib improves progression-free survival (PFS) as sequential therapy after platinum-doublet chemotherapy [17]. The Phase III IRESSA NSCLC Trial Evaluating Response and Survival Against Taxotere (INTEREST) and V-15-32 studies comparing gefitinib and docetaxel in unselected pretreated patients showed no difference in OS, suggesting that gefitinib and docetaxel were equally effective as the second-line therapy [18,19]. In addition, the Phase III IRESSA Pan-Asia study (IPASS) comparing gefitinib monotherapy with carboplatin/paclitaxel showed an improved PFS time in the gefitinib arm [20]. On the other hand, molecular studies have revealed that EGFR-activating mutations and high *EGFR* gene copy number are frequently found in patients who have the best outcomes with EGFR TKIs [21–27]. Currently, investigators are trying to determine the optimal approach to selecting patients for treatment with EGFR TKIs. Gefitinib is the first class of oral targeted therapies to produce such responses in advanced NSCLC and the most studied agent in clinical trials.

Chemistry

Gefitinib, 4-(3-chloro-4-fluoroanilino)-7-methoxy-6-(3-morpholinopropoxy) quinazoline (ZD1839, IRESSA; Figure 1), is an orally active, low-molecular-weight (447 kDa) quinazolin derivative

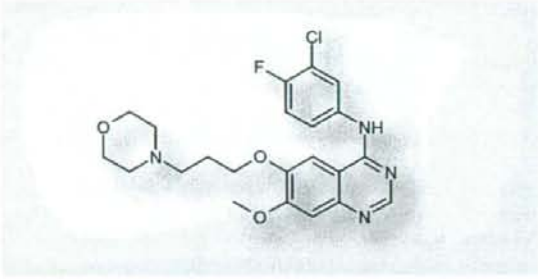

Figure 1. Gefitinib.

with a molecular formula $C_{22}H_{24}ClFN_4O_3$ that specifically inhibits the activation of EGFR tyrosine kinase through competitive binding of the ATP-binding domain of the receptor.

It is readily soluble at pH1 and highly insoluble above pH7. Gefitinib is very stable at room temperature with a proven shelf-life of 36 months [28].

Pharmacodynamics

Gefitinib selectively inhibits the activation of EGFR tyrosine kinase through competitive binding of the ATP-binding domain of the receptor. Selectivity was demonstrated versus HER2 and the VEGF tyrosine kinases, kinase insert domain receptor and Flt-1, with at least a 100-fold difference in IC_{50} for EGFR compared with other tyrosine kinases. Similarly, gefitinib did not inhibit the activity of the serine threonine kinases raf, MEK-1 and ERK-2 (MAPK) [29]. In the Phase I trials, the maximum tolerated dosage was 700 mg/day, although dosages as low as 150 mg/day provided plasma concentrations sufficient for pharmacological activity, evidence of targeted biological effect and anti-tumor activity [30–33]. An analysis of pharmacodynamics marker levels in the skin also provided evidence that sufficient gefitinib was reaching the skin and inhibiting EGFR signaling at 150 mg/day [34]. Additionally, objective tumor responses observed across a dosage range of 150–1000 mg/day indicated that these dosages resulted in target inhibition in tumors. Two large Phase II trials (IDEAL-1 and -2) evaluated 250- and 500-mg/day dosages of gefitinib in patients with advanced NSCLC. As predicted from the Phase I trials, dosages of more than 250 mg/day provided no additional efficacy benefit, whereas adverse effects increased in a dose-dependent manner. Consequently, the recommended dose of gefitinib in NSCLC is 250 mg/day [10,11]. Pharmacodynamic studies indicate that gefitinib blocks cell cycle progression in the G_1 phase by upregulating $p27^{Kip1}$, a cell cycle inhibitor, and downregulating c-fos, a transcriptional activator that is prominent in EGFR-mediated signaling [35]. Elevated levels of $p27^{Kip1}$ block cell cycle progression in the G_1 phase of growth. This sustains the hypophosphorylated state of the *Rb* gene product, which is necessary to keep cells from progressing in the cell cycle [36]. The inhibition of tumor growth seen with gefitinib is also accompanied by decreases in VEGF, basic FGF and TGF-α, all potent inducers of tumor angiogenesis [37]. Thus, gefitinib may also inhibit tumor growth by interfering with angiogenesis. These observations suggest that by inhibiting the EGFR tyrosine kinase, gefitinib treatment alters expression levels of key molecules in tumor cells that are important for stimulating proliferation, cell cycle progression, tumor angiogenesis, metastasis and inhibition of apoptosis. Gefitinib treatment can also cause apoptosis to occur *in vitro*, the frequency of which correlates with the cell line sensitivity to the drug and provides a link with the tumor shrinkage reported clinically [38].

Pharmacokinetics & metabolism

The pharmacokinetic profile revealed that gefitinib is orally bioavailable and suitable for once-daily dosing in cancer patients. In healthy volunteer studies, gefitinib was absorbed moderately slowly, reaching C_{max} 3–7 h after administration. The elimination half-life of 28 h suggests that once-daily oral administration is appropriate [34]. In the initial Phase I studies of gefitinib, sequential skin biopsies were performed prior to and after 4 weeks of therapy [34]. The skin was selected as the target tissue due to its easy access and the established role of the EGFR in renewal of the dermis. Inhibition of EGFR phosphorylation and EGFR-dependent downstream processes was detected at dosages of 150 mg/day, well below the maximal tolerable dosage (MTD) of 700 mg/day. In a clinical study (BCIRG 103), gefitinib (250 mg) was administered orally to breast cancer patients for at least 14 days [39]. Gefitinib concentrations in each tumor sample (mean: 7.5 µg/g) were substantially higher (mean: 42-fold) than the corresponding plasma sample (mean: 0.18 µg/ml). Haura *et al.* conducted a pilot Phase II study of a 28-day preoperative course of gefitinib 250 mg orally, followed by surgical resection for patients with stage IA to selected IIIA NSCLC [40]. Tumor penetration of gefitinib was assessed in surgically resected tumor samples along with plasma assessment on day 28. Day 28 plasma concentrations of gefitinib averaged 531 ± 344 nM (range: 65–1211 nM) while tumor concentrations of gefitinib averaged 33,108 ± 44,312 nM (range: 74–134,669 nM). These results also demonstrate that NSCLC tumor penetration of gefitinib is high, as its tumor concentrations were much higher than concentrations found in plasma.

Gefitinib is metabolized extensively by expressed cytochrome P450 (CYP)3A4, producing a similar range of metabolites to liver microsomes, while CYP3A5 produced a range of metabolites, similar to CYP3A4 but to a much lower degree [41,42]. By contrast, CYP2D6 catalyzed rapid and extensive metabolism of gefitinib to desmethyl-gefitinib (M523595). While formation of M523595 was CYP2D6 mediated, the overall metabolism of gefitinib was dependent primarily on CYP3A4. Quantitatively, the most important routes of gefitinib metabolism were mediated primarily by CYP3A4, while CYP3A5 and CYP2D6 were minor contributors. The wide variability in CYP3A4 activity in human liver is probably a significant factor in the interindividual variability observed in gefitinib pharmacokinetics. Gefitinib has interactions with CYP3A4 inducers, or CYP3A4 enzyme inhibitors or substrate of CYP2D6 (gefitinib inhibits CYP2D6 activity) or H2 blockers. Pharmacokinetic studies have shown that the bioavailability of gefitinib is unaffected by food intake to any clinically significant extent [43].

Clinical efficacy

Several challenges were encountered in designing the clinical trials of gefitinib, because this agent was expected to be cytostatic rather than cytotoxic. These challenges included a scarcity of precedents, the way in which 'biological activity' was defined, the integration of outcomes across multiple tumor types in Phase I trials, the relationship between biological activity and clinical outcome, and unknown pharamakokinetic and pharmacodynamic relationships. Initially, clinical trials of gefitinib were performed principally in unselected patient populations with NSCLC. However, recent results indicate that different patients derive different degrees of clinical benefit from treatment with gefitinib. The identification of the patients who are most likely to derive clinical benefit from gefitinib is of paramount importance.

Phase I

As biologically targeted agents are expected to provide clinical benefits that are not predicted by surrogate end points of toxicity to normal replicating tissue, new Phase I trials have been designed to determine the optimum biological dose for use in further studies. Initial Phase I trials performed in healthy volunteers showed that oral administration of gefitinib given once on day 1 (50, 100, 250 or 500 mg) or daily for 14 days (100 mg/day) was feasible [44]. Four multicenter Phase I trials then evaluated the safety profile of gefitinib (50–1000 mg/day) in more than 250 patients with a wide range of solid tumors that were known to express EGFR, although baseline EGFR expression levels were not determined [30–32,45]. Adverse events (AEs) occurred at dosages of 50 mg/day, with the most commonly reported AEs being mild-to-moderate acne-like rash, diarrhea, nausea, anorexia, vomiting and asthenia. The frequency of AEs, such as skin rash and diarrhea, increased with dose, and the MTD was identified as 700 mg/day. Clinical benefit was not dose-related, whereas the most common AEs (skin rash and acne) increased with gefitinib dose. In addition, pharmacokinetic studies indicated that plasma levels of gefitinib over this dose range were sufficient for effective EGFR inhibition. Although the lowest dose at which objective tumor responses were observed was 150 mg/day, there was potential for individuals receiving this dose to have subtherapeutic exposure as a result of interpatient variability in pharmacokinetics. Accordingly, the slightly higher dosage of 250 mg/day was chosen. The second dosage chosen was 500 mg/day, which was the highest dosage that was well tolerated by most patients on a daily dosing schedule. Both dosages were significantly lower than the MTD, unlike conventional dosage selection for chemotherapy agents, which would use the MTD.

Phase II

Large-scale dose-evaluation study

Two large, dose-randomized, double-blind, parallel-group, multicenter Phase II trials (IDEAL-1 and -2) independently evaluated the activity of gefitinib 250 and 500 mg/day in 425 patients with advanced NSCLC [10,11]. These trials allowed a more detailed evaluation of the doses selected from the Phase I trials and included symptom improvement as an additional end point. In IDEAL-1, conducted mainly in Europe and Japan, patients with one or two prior chemotherapy regimens, including a platinum compound, were randomly assigned to receive gefitinib at 250 or 500 mg/day. Response rate approached 20% and was similar in both arms, and symptom improvement was 40%, which was higher in patients who had an objective response. Adverse effects were, in general, well tolerated, but were more severe with the 500-mg dose. In IDEAL-2, the study was performed in 30 centers in the USA. In total, 221 patients were randomly assigned to receive either gefitinib 250 or 500 mg daily. A total of 126 patients (58%) had three or more regimens in the past and 65% had histology of adenocarcinoma. Symptoms of NSCLC improved in 43% of patients receiving gefitinib 250 mg and in 35% of those receiving 500 mg. There was no significant difference in response rate or survival between the two doses. There was a good correlation between clinical response and symptomatic improvement. However, the gefitinib 500-mg dose was more toxic as it induced more acne-like rash and diarrhea. In conclusion, gefitinib was well tolerated at 250 mg/day and it induced anti-tumor activity in approximately 10% of patients. These results are impressive compared with chemotherapy, which induces far more adverse effects and, probably, even a lower level of activity.

Gefitinib as first-line treatment

In East Asia, Phase II trials of gefitinib as first-line therapy have demonstrated good response rates of 30% compared with those in patients of non-East Asian origin (<10%) [46–51]. In a prospective Phase II trial of chemotherapy-naive patients with advanced NSCLC conducted in Japan, 40 patients treated with first-line gefitinib were evaluated for response. Partial response was seen in 12 (30%) patients [47]. Response to gefitinib in studies of non-Asian patients have been shown to be much lower than in studies of Asian patients. In a study in the USA, response rate among 70 patients with advanced NSCLC and poor performance status (2 or 3) was 4% [50]. In Germany, response rate among 58 patients with inoperable advanced NSCLC and good performance status (0–2) was 5% [49]. Results from IRESSA in NSCLC versus Vinorelbine Investigation in the Elderly (INVITE) reported no statistical difference between gefitinib and chemotherapy first-line for median PFS rates (2.7 vs 2.9 months, respectively) or overall response rates (3.1 vs 5.1%, respectively) [52,53]. Iressa NSCLC Trial Evaluating Poor Performance Patients (INSTEP) reported a response rate of 6% and a trend toward improved efficacy end points with gefitinib first-line compared with placebo, with similar improvements in quality of life and symptoms in Western patients with poor performance status [54]. See Table 1 for a detailed list.

Gefitinib therapy in selected patients

Table 2 lists several reports on gefitinib sensitivity in selected patients [55–66]. In 2004, several investigators reported that somatic mutations in the gene for the EGFR [21–23], the targets

Table 1. Phase II studies of gefitinib.

Author/study	Treatment arms	Number	ORR (%)	PFS (months)	MST (months)	Comments	Ref.
Gefitinib in the second- and third-line treatment of advanced NSCLC							
Fukuoka *et al.* (IDEAL-1)	Gefitinib 250 mg daily	103	18.4	2.7	7.6*	Randomized Phase II trial conducted mainly in Europe and Japan	[10]
	Gefitinib 500 mg daily	105	19.0	2.8	8.0		
Kris *et al.* (IDEAL-2)	Gefitinib 250 mg daily	102	12.0	NA	7.0**	Randomized Phase II trial conducted in the USA	[11]
	Gefitinib 500 mg daily	114	9.0		6.0		
Gefitinib in the first-line treatment of patients with NSCLC							
Goss *et al.* (INSTEP)	Gefitinib	100	6.0			Randomized Phase II trial in patients with poor performance status; modest benefit seen with gefitinib	[54]
	Placebo	101	1.0				
Crino *et al.* (INVITE)	Gefitinib	97	3.1	2.7		Randomized Phase II trial in elderly patients; similar efficacy observed	[52]
	Vinorelbine	99	5.1	2.9			
Niho *et al.*	Gefitinib 250 mg	40	30.0	NA	13.9		[47]
Lin *et al.*	Gefitinib 250 mg	53	32.1	3.2	9.4		[46]
Suzuki *et al.*	Gefitinib 250 mg	34	26.5		14.1		[48]
Reck *et al.*	Gefitinib 250 mg	58	5.0	1.6	6.7		[49]
Spigel *et al.*	Gefitinib 250 mg	70	4.0	3.7	6.3	Patients with poor performance status	[50]
Swinson *et al.*	Gefitinib 250 mg	41	10.0	1	2.7	Patients unsuitable for chemotherapy	[51]
Gefitinib compared with docetaxel in the second-line treatment of advanced NSCLC							
Cufer *et al.* (SIGN)	Gefitinib 250 mg	68	13.2	3.0	7.5***	Open label,randomized Phase II study; fewer drug-related side effects with gefitinib	[114]
	Docetaxel 75 mg/m²	73	13.7	3.4	7.1		

*p = NS.
**p = 0.40.
***p = 0.88.
HR: Hazard ratio; IDEAL: IRESSA Dose Evaluation in Advanced Lung Cancer; INVITE: Iressa in NSCLC versus Vinorelbine Investigation in the Elderly; MST: Median survival time; NA: Not available; NS: Not significant; NSCLC: Non-small-cell lung cancer; ORR: Overall response rate; PFS: Progression-free survival.

of gefitinib, were associated with dramatic and durable regressions with gefitinib in patients with NSCLC. To confirm the encouraging but retrospective results of early studies, multiple groups undertook prospective Phase II trials of gefitinib in patients found to have an *EGFR* mutation on screening. To date, at least nine studies have been reported [55-63]. Collectively, these showed that nearly 80% of patients whose tumors had either exon 19 deletions or L858R mutations had radiographic responses to gefitinib, although responses varied between different trials. The combined analysis of seven prospective trials conducted in Japan, which examined the efficacy and safety of gefitinib monotherapy for NSCLC with *EGFR* mutations, has been reported. In this study, Morita *et al.* updated OS and PFS data for the combined survival analysis and examined prognostic factors for OS and PFS (J-CAMP study) [67]. A total of 148 patients were combined from the seven trials and median OS and PFS of 24.3 months and 9.7 months weer reported, respectively. The combined response rate was 76.4%, and only 6% of the patients had progressive disease. They concluded that gefitinib produces significant anti-tumor activity and prolonged survival in this selected NSCLC population. A prospective Phase II study has also demonstrated that gene copy number assessed by fluorescent *in situ* hybridization (FISH) [25] may predict clinical outcome in TKI-treated NSCLC patients. In advanced bronchioloalveolar carcinoma, a distinct subtype of adenocarcinoma, gefitinib was clinically active in both chemotherapy-naive and pretreated patients [65,66].

Phase III

Gefitinib in combination with chemotherapy

The IRESSA NSCLC Trial Assessing Combination Treatment (INTACT)-1 and -2 studies were large randomized studies of two dosages of gefitinib (250 or 500 mg/day), or placebo, in combination with two different chemotherapy regimens [13,14]. INTACT-1 used cisplatin and gemcitabine (cisplatin 80 mg/m² on day 1 and gemcitabine 1250 mg/m² on days 1 and 8 every